Prepared for the National Institutes of Health
National Institute of Neurological Disorders and Stroke
Division of Fundamental Neurosciences
Neural Prosthesis Program
Bethesda, MD 20892

Unassisted Standing with Functional Neuromuscular Stimulation

NIH-NINDS-N01-NS-6-2351

Progress Report #5

Period Covered:
January 1, 1998 – March 31, 1998

Principal Investigator: Ronald J. Triolo, Ph.D.[1]
Co-Principal Investigators: Robert F. Kirsch, Ph.D.[2]
John A. Davis, Jr., M.D.[1]

Departments of Orthopaedics[1] and Biomedical Engineering[2]
Case Western Reserve University
Cleveland, OH 44106-4912

Co-Investigators: James J. Abbas, Ph.D.
University of Kentucky

Scott L. Delp, Ph.D.
Northwestern University

I. INTRODUCTION

The long-term goal of this contract is to develop methods to provide brace-free, energy efficient standing for persons with complete thoracic level spinal cord injuries via functional neuromuscular stimulation (FNS). The resulting system will resist reasonable disturbances and maintain balance automatically while allowing free use of the upper extremities to manipulate objects in the environment. These objectives are being addressed through an organized effort consisting of anatomical and dynamic modeling, control simulation and optimization, and experimental demonstration of new control structures. The work represents an active partnership between investigators at Case Western Reserve University (CWRU) and collaborators at Northwestern University and the University of Kentucky.

Achieving independent, hands-free standing with FNS depends upon the developing an anatomically realistic and dynamic model of the lower extremities and torso. This model will be employed to conduct dynamic simulations and perform optimization procedures to investigate the theoretical behavior of various FNS control systems for providing automatic postural adjustments. Over the last quarter, substantial progress has been made in a) modeling the musculoskeletal anatomy of the trunk, b) estimating the postural disturbances generated by voluntary movements of the upper extremities, and c) adapting the model of the lower extremities to account for the affects of FNS and spinal cord injury (SCI). This report summarizes these results and their relationship to the overall goals of the contract.

III. PROGRESS THIS REPORTING PERIOD

Progress this reporting period was made primarily in the following areas: 1) anatomical modeling of the torso, 2) biomechanical modeling and simulation. The latter includes computing the disturbances due to volitional arm movements, and adjusting model parameters to reflect experimental data obtained from stimulated paralyzed muscle.

A. Anatomical Modeling of the Torso

A second set of experiments were performed on another cadaver specimen to analyze trunk muscles in detail and determine their architectural and morphometric parameters. The cadaver was dissected at MetroHealth Medical Center (Cleveland, OH) and detailed notes, diagrams, and photographs of the intact muscles were taken. The columns of the *erector spinae* (*spinalis thoracis, longissimus thoracis, and illiocostalis lumborum*), the *quadratus lumborum*, and the *rectus abdominus* were harvested. Photographs and measurements were taken from the detached muscles and markers were placed on key attachment locations according to the same protocol used for the first specimen as described in Quarterly Progress Reports 3 & 4. The muscles were preserved in formalin and transferred to Northwestern University in (Chicago, IL) for further analysis.

Important architectural and morphometric parameters such as musculotendon length, muscle length, pennation angle, average fiber length, and average sarcomere length were obtained from each muscle. The optimal fiber length and the physiological cross-sectional area (PCSA) were also calculated. **Table I** summarizes these measurements for the most recent specimen.

Table I Summary of muscle parameters obtained from the most recent cadaver specimen

MUSCLE	MT	ML	PA	AFL	ASL	OFL	PCSA
Proximal Quadratus Lumborum	11.4	11.0	4	9.06 ± 0.75	2.65 ± 0.03	9.56 ± 0.79	1.09
Distal Quadratus Lumborum	9.6	9.1	0-5	5.05 ± 0.31	2.57 ± 0.04	5.49 ± 0.35	1.27
Spinalis Thoracis	26.0	21.0	15	4.75 ± 0.71	2.39 ± 0.06	5.56 ± 0.74	3.38
Longissimus Thoracis	48.0	42.5	14	9.86 ± 0.96	2.36 ± 0.03	11.71 ± 1.06	6.58
Illiocostalis Thoracis	47.0	42.0	10	14.2 ± 1.01	2.39 ± 0.23	16.64 ± 1.12	2.44
Rectus Abdominus	39.0	38.3	0	34.52 ± 0.49	3.12 ± 0.11	31.72 ± 0.57	1.97

MT: Musculotendon length (cm)
ML: Muscle length (cm)
PA: Pennation Angle (degrees)
PCSA: Physiologic cross-sectional area (cm^2)
ASL: Average sarcomere length (μm)
OFL: Optimal fiber length (cm)
AFL: Average fiber length (cm)

Table II Summary of muscle parameters obtained from the previous cadaver specimen

MUSCLE	MT	ML	PA	AFL	ASL	OFL	PCSA
Proximal Quadratus Lumborum	10.9	10.5	7	6.24 ± 0.44	2.99 ± 0.11	5.41 ± 0.95	1.03
Distal Quadratus Lumborum	8.5	8.4	0-5	4.24 ± 0.90	2.90 ± 0.14	4.08 ± 0.76	0.83
Spinalis Thoracis	25.0	14.0	18	5.22 ± 1.06	2.51 ± 0.05	5.82 ± 1.12	0.80
Longissimus Thoracis	37.6	31.1	22	10.1 ± 0.78	2.46 ± 0.04	11.38 ± 1.00	3.39
Illiocostalis Thoracis	37.6	28.5	10	11.97 ± 0.62	2.47 ± 0.06	13.57 ±0.73	3.03
Rectus Abdominus.	34.3	33.0	0	28.0 ± 0.67	3.62 ± 0.08	21.67 ± 0.59	1.75

Table II lists the values for the same parameters that were obtained from the previous cadaver specimen. All the muscles from the most current specimen were longer (musculotendon length) than those obtained from the first cadaver. The pennation angles were very similar, indicating the muscle fibers are arranged consistently across different subjects. The *rectus abdominus* showed long sarcomere lengths (> 3.0 μm) in both cadavers. The sarcomere lengths for the other muscles of the most recent specimen were in the range of 2.4 - 2.7 μm and were

consistent with those found in the first specimen (range 2.3 - 2.9 μm). The PCSAs obtained for *quadratus lumborum*, *illiocostalis lumborum*, and *rectus abdominus* were consistent across specimens. However, the values for PCSA of the *spinalis thoracis* and *longissimus thoracis* from the second cadaver were significantly larger than those obtained from the first cadaver. This could be due to naturally occurring individual variation, or to the dissection technique which might have included some fibers from the *multifidus* muscle with the samples from the second specimen.

Variation of muscle parameters from one subject to another is a major concern in modeling a muscle's force generating capacity. For this reason, we plan to measure muscle parameters from 3-4 more specimens in order to determine the range of values for each of the muscle parameters.

In summary, over the past year we have a) scaled a digitized representation of the vertebral column, b) compared antrhopometric parameters of each vertebra with data published in the literature, c) integrated the scaled representation of the spine into the existing lower extremity model, d) verified the overall model by comparing selected antrhopometric parameters with published data, e) defined preliminary models of the spinal muscles based on anatomy texts and preliminary cadaver studies, f) completed a preliminary comparison of muscle moment arms with published CT/MRI data, g) harvested trunk muscles from two cadaver specimens, h) measured architectural and morphometric parameters for each muscle, and i) refined the preliminary model of the muscles based on the detailed analysis of the two specimens.

B. Biomechanical Modeling and Simulation

In previous reports we described the development of a dynamic, three-dimensional, closed-chain model of the two human lower extremities and demonstrated the feasibility of using it to perform control simulations. This bipedal model consists of the lower extremities, pelvis, and a first approximation of the torso. However, the upper extremities are not represented. Postural disturbances due to upper extremity movements are input into the simulations as forces and moments applied to the shoulder. We have developed techniques to estimate the postural disturbances caused by volitional upper extremity movements, which have been described in earlier progress reports. Over the last three months we have completed the experimental verification of this element of the model with able-bodied subjects, and have begun to compile a catalog of force and moment records representative of functional arm movements. An automatic control system to maintain balance will need to compensate for these types of disturbances. During the current reporting period we have also continued to identify ways to make the model more realistic by incorporating the behavior of paralyzed muscle to electrical stimulation, rather than relying on the default able-bodied parameters. To this end we have completed a preliminary analysis to optimize the Hill-type muscle model to reflect experimentally measured isometric moments about the hip.

Estimating postural disturbances resulting from voluntary arm movements: Work on the development and experimental validation of a three-dimensional biomechanical model of the upper extremity has been completed. As stated in earlier progress reports, the upper extremity was represented as three rigid segments joined by gimbal joints at the shoulder and elbow, and a solid weld joint at the wrist. The elbow was gimbaled to represent pronation/supination and the carrying angle of the arm. Segment masses and locations of moments of inertia were calculated from regression equations based on standard anthropomorphic measurements. Dynamic

calculations were performed offline to solve for the forces and moments at the shoulder joint given kinematic measurements of the segment positions in space. Efforts this quarter have focussed on experimental validation of the model.

Six able-bodied subjects, five male and one female, volunteered to take part in the validation experiments. Each subject performed two types of unimanual arm movements and one bimanual task. The first set of unimanual movements was planar. Each subject was instructed to move his or her right arm through one of the three anatomical planes (sagittal, coronal or transverse) with the elbow held in full extension. Each of the three planar movements was conducted under four conditions: 1) slow unloaded, 2) slow loaded, 3) fast unloaded, and 4) fast loaded. The load was a 2.268 kg weight held in the hand. A metronome, set at 45 beats per minute, was used to help the subject achieve a uniform movement rate. The slow movements were performed at a rate of four beats per cycle (11.25 cycles per minute), and the fast movements were performed at twice that rate. For the second set of unimanual tasks, the subject was instructed to make random, self-paced movements that included elbow flexion and extension. Loaded and unloaded trials were conducted, using the same five-pound weight.

For all unimanual tasks, the subjects were seated on two AMTI force platforms to validate the model. The subject was instructed to prevent movement of his or her head and trunk so that the true shoulder reactions could be accurately computed from the force platform data. The recorded ground reaction forces and moments were transformed into reaction loads acting at the shoulder for comparison with the output of the inverse dynamics model. The difference between the modeled and externally measured reaction loads was calculated, and a root mean squared error (RMS) value was found for each trial. The average RMS error values over all of the trials was 2.4 N for the forces and 1.52 N-m for the moments.

The typical output of the model and reaction loads recorded by the force platforms for a fast, unloaded transverse movement are shown in **Figure 1**, along with the RMS errors for each data set. As described in previous reports, the global X-axis points anteriorly, the Y-axis points superiorly, and the Z-axis points laterally. As **Figure 1** demonstrates, there is good agreement between the measured values and those estimated with the upper extremity model. Since the transverse movement occurs in the XZ-plane, the force disturbances in that direction are greatest. The Y-axis forces are offset by approximately 60 N due to the weight of the arm segments and the hand load. The moment about the Y-axis occurs because it is the axis of rotation of the arm system. For coronal and sagittal movements, the moment about the axis of rotation is the only one that is present, but transverse movements are unique because of the additional moments that are generated about the other two axes due to the force of gravity acting on the arm segments. The X-axis moments go from positive to negative as the arm crosses the axis, and the magnitude of the Z-axis moments decrease as the arm moves toward the axis and increase as the moment arm of the force of gravity becomes larger.

The bimanual task was chosen to represent a typical functional activity. Subjects performed the movements while standing at a counter 88 cm high, and were instructed to repeatedly move the five pound weight from one location to another. The weight was held in the mid-sagittal plane, and the movements were assumed to be perfectly symmetrical, with each arm supporting half of the load. Data were collected for each of three movements: 1) lifting the weight from the counter to a low shelf (40 cm above the counter), 2) from the counter to a higher shelf (61 cm above the counter), and 3) from the lower shelf to the higher shelf. The edges of the shelves were 36 behind the front edge of the table. The subjects were instructed to stand with their toes even with the front edge of the table and their bodies aligned with the table. Results

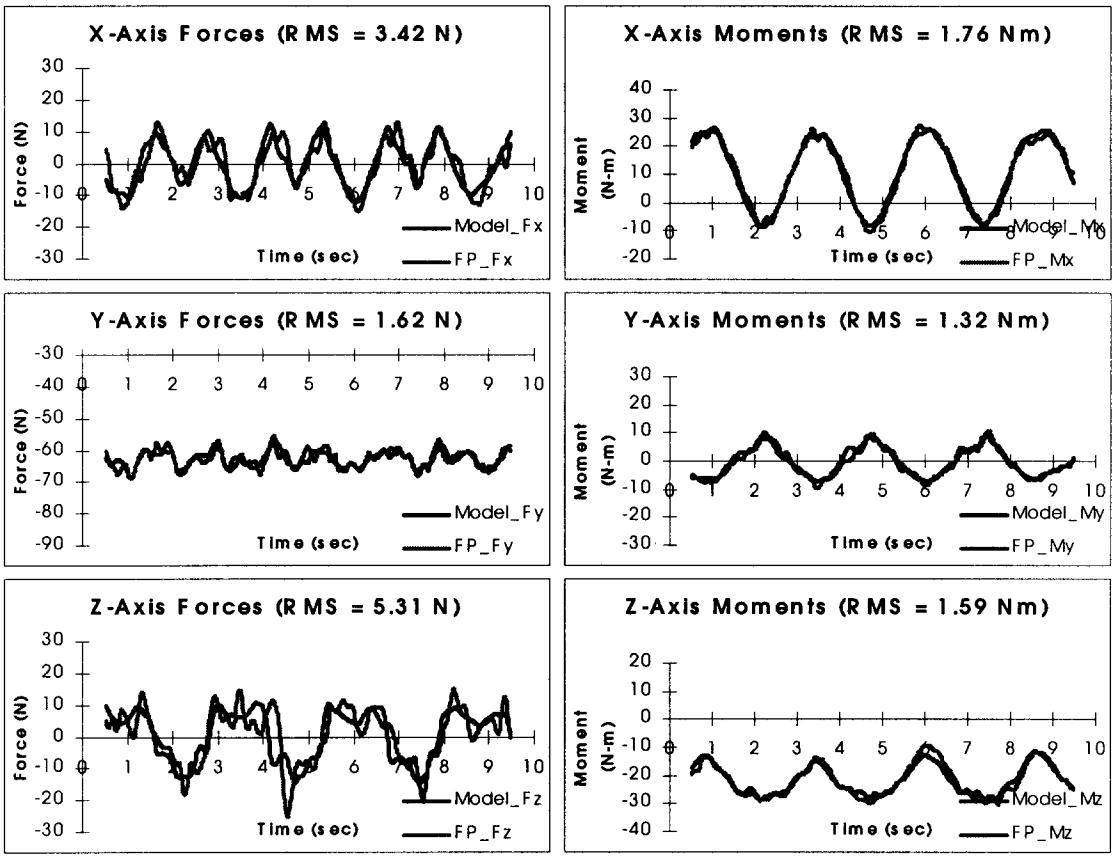

Figure 1: Typical results of validation experiments with fast, unloaded unimanual movements in the transverse plane. Note good agreement between model estimates of shoulder forces and moments (Model_Fx, etc.) and those measured by the force platforms (FP_Fx, etc.). RMS errors are noted for each reaction component.

from a typical bimanual task are shown in **Figure 2**. For this trial, the subject was moving the weight from the counter to the higher shelf. The top chart shows the height of the subject's hands over the course of the movement.

The results depicted in **Figure 1** and **Figure 2** are representative of those collected from all six subjects. The upper extremity model performed well across all subjects, and successfully accounted for the large variations in their height and weight. The consistency of performance indicates the robustness of the approach.

In summary, the experimental measurements closely approximated the output of the model, verifying the technique. Fast, loaded movements produced the largest forces and moments at the shoulder in all cases and would be the most destabilizing to posture and balance. Future plans for this phase of the project include the collection of kinematic data from additional types of arm movements and functional activities, including reactions to unexpected changes in load. These data will be compiled to form a catalog of the types of disturbances that are likely to be encountered during standing. A similar model of the left arm could also be developed later for use in the study of non-symmetrical bimanual tasks.

Two abstracts summarizing this portion of the project have been accepted for presentation at scientific meetings and conferences. The first abstract was awarded first prize in the scientific

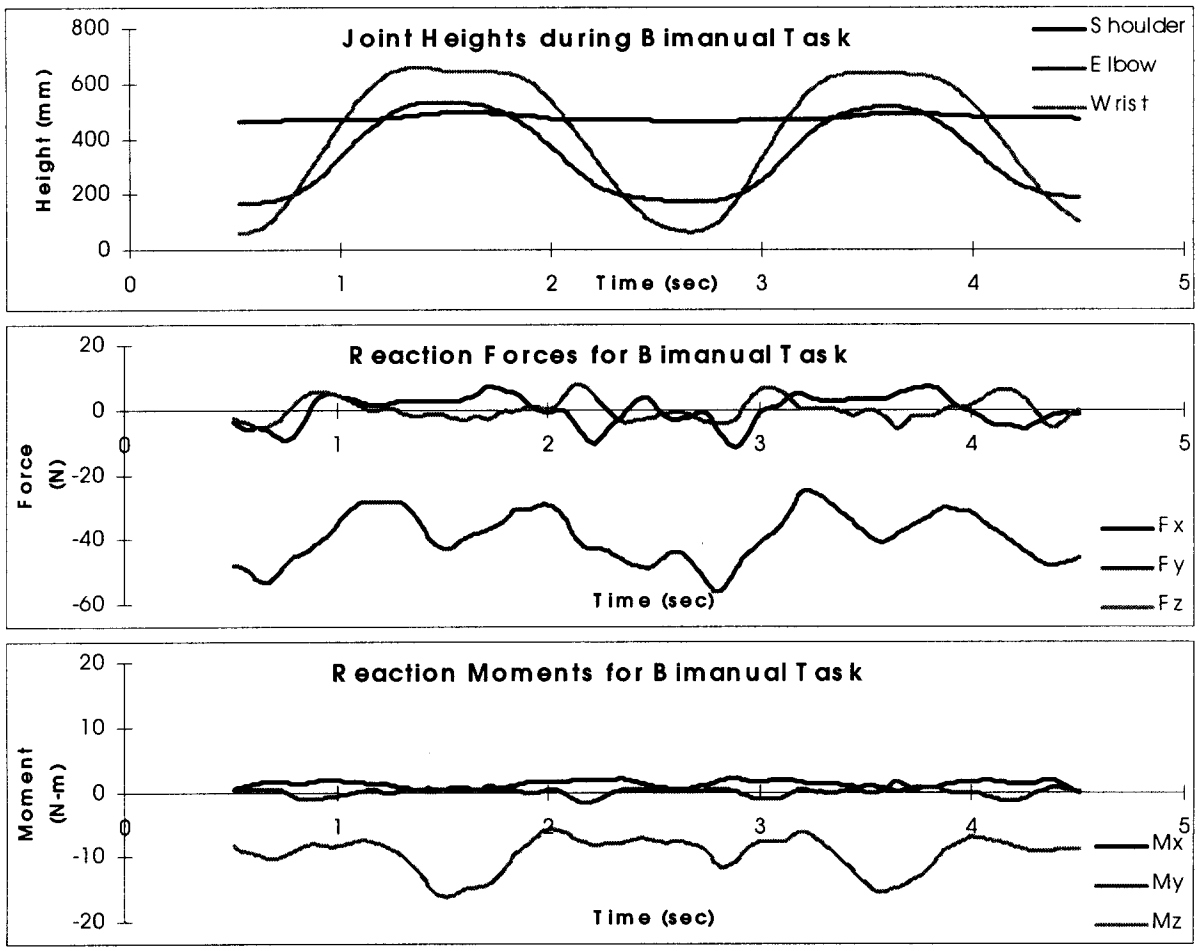

Figure 2: Representative results from bimanual lifting task involving moving a 2.268 kg load from a 34.5" counter to a shelf 24" above and 14" anterior to its original location.

paper competition at the Rehabilitation Engineering Society of North America annual meeting (Minneapolis MN, June 1998), and the second will appear in the proceedings of the Fifth International Symposium on the 3-D Analysis of Human Movement. We are currently preparing a paper for publication in a peer-reviewed journal on this topic.

Adjusting muscle model parameters for chronic SCI and FNS: The musculoskeletal model of human lower extremities used as a tool to design strategies and to select muscles to restore standing with FNS is based on an able-bodied specimen of average height and weight. The parameters of the muscle model do not currently account for the recruitment properties of stimulating electrodes, or changes in the moment generating capacity of lower extremity muscles after long term SCI. The objective of this part of the study is to characterize the physiological changes following the injury so that the muscle model parameters can be adjusted to more accurately reflect the actions of FNS in individuals with chronic SCI who are the target users of the standing neuroprosthesis.

Atrophy or loss of muscle mass has been identified in chronic SCI individuals due to lack of use and muscle denervation subsequent to motorneuron loss. The effects of atrophy can be modeled as a reduction in PCSA, and therefore a reduction in the maximum force produced by

the muscle. Full recruitment of all motor units may also be impossible with FNS due to variations in the position of stimulating electrodes and their effectiveness in fully exciting all the neural tissue innervating a muscle. This would also tend to decrease the maximum muscle force. Long-term immobilization can alter the length of the musculotendon complex, and hip flexion and other types of contractures are common in the SCI population. Prolonged sitting could result in stretching or shortening of the muscle fibers or connective tissues.

For these reasons, we chose to adjust the parameters of the muscle model corresponding to peak isometric force (f^m_o), fiber length (l^m_o) and tendon length (l^t_s) to match the isometric moments produced by the hip extensor muscles with FNS in volunteers with chronic SCI.

The isometric strength of hip extensor muscles (*gluteus maximus*, *semimembranosus*, and posterior portion of the *adductor magnus*) from five individuals with chronic SCI were measured at five discrete hip angles using an instrumented CYBEX II Dynamometer. Subjects were well-conditioned and active participants in other standing research projects. With subjects lying supine and tightly strapped to prevent any pelvic motion, the hip was positioned at 5 discrete angles approximately 18° apart between full-extension and 90° of flexion. Testing was performed with the knee fully extended and locked in position by a brace. Steady-state moments were measured during repeated 5 second tetanic contractions generated by a 20 mA, charge-balanced, asymmetric, bi-phasic stimulus with inter-pulse-interval of 30 msec. Stimulus bursts were delivered intermittently (duty cycle of 1:8) to the muscles in random order to avoid fatigue. The pulse durations were set for each muscle to the maximum values before spillover to an adjacent muscle or unwanted reflex activation. Order of stimulation was randomized and long on:off ratios were used to avoid fatigue.

Two optimization searching algorithms, Simplex and Quasi-Newton (The Mathworks, Inc.), were employed to adjust musculotendon actuator model parameters (i.e., fiber length and peak isometric muscle force) so that the predictions from the model can be matched with the measured results with a minimum discrepancy. Both searching algorithms generated very similar results, although the Quasi-Newton method generally converged faster. Furthermore, since the searching problem is very nonlinear, the obtained solution may be optimal only in a local sense. To increase the chance that the solution is globally optimal, different initial guesses were used in the searches and contours of matching error as a function of the model parameters were generated. As an example, the matching error contour for the *semimembranosus* is plotted in **Figure 3** as a function of fiber length and peak isometric muscle force. The plot indicates that a global optimum may exist in this case.

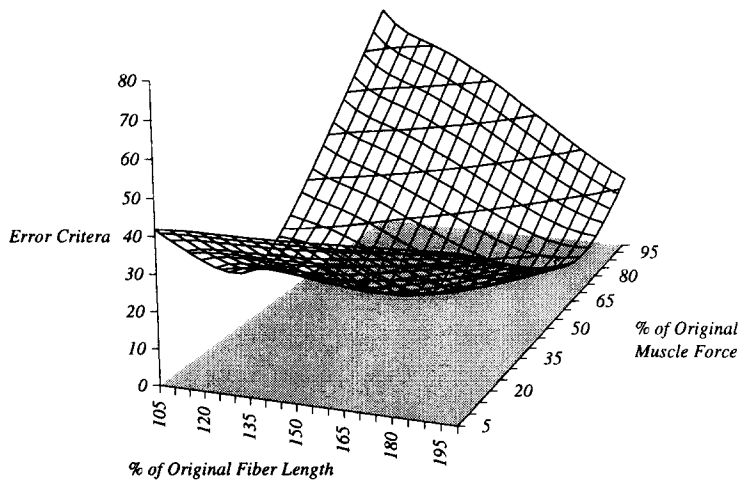

Figure 3: Error between predicted and measured values of isometric hip extension moment for semi-membranosus as a function of model parameters.

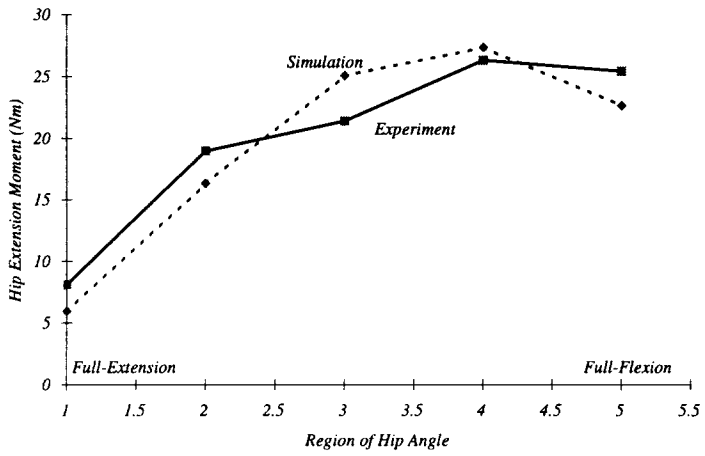

Figure 4: Isometric hip extension moment produced by stimulation of the semimembransosus, and the best match obtained by varying muscle model parameters (peak isometric force f^m_o, and fiber length l^m_o).

Figure 4 shows the experimentally measured isometric hip extension moments for the *semimembranosus* along with the output of the model with parameters adjusted to minimize the error. In this case, isometric peak force was decreased and fiber length was increased by factors corresponding to the entries in **Table 3**.

The optimal solutions (those providing minimum error between the simulated and measured moment) for all the muscle model parameters taken individually and in combination are summarized in **Table 3.** The optimal results are given as a percentage of change from the initial able-bodied muscle parameters. The errors resulting from adjusting more than one muscle parameter simultaneously were less than the those derived from adjusting only one muscle parameters, as shown in **Table 4.** This suggests that the physiological changes following SCI and the actions of FNS simultaneously affect more than one muscle parameter. Furthermore, the minimum errors for *gluteus maximus* and *semimembranosus* were obtained by simultaneously decreasing the peak isometric force by approximately 50%, and increasing the fiber length parameters. However, the optimal solution for the posterior portion of the *adductor magnus* involves a shortening of the fibers, rather than a lengthening as in the other cases. This may be due to the fact that in the sitting position, the adductor muscles are in a shortened position, while the other hip extensors are lengthened.

The next step in this phase of the study is to restrict the changes in muscle model parameters to remain within anatomical and physiological limits. Similar analyses can then be performed for other key muscle groups for standing with FNS (such as the quadriceps). Direct measurement of the model parameters with FNS in the SCI population will also be explored.

Immediate plans for the next contract period include initiation of experimental procedures to validate the three-dimensional closed-chain dynamic bipedal model of standing with able-bodied volunteers. We also plan to quantify the effects of stimulated hip extension moment and posture on arm support forces in volunteers with SCI who are currently standing with FNS. This will address one of our stated goal of characterizing standing with open-loop stimulation in order to better understand the role of automatic postural control systems. Efforts to quantify the passive properties of the joints of the lower extremities will continue as we proceed to refine our computer model and simulations to represent SCI and the effects of FNS.

Table 3: Relative changes in muscle model parameters yielding optimal match to experimental data

Model Parameter	Muscle		
	Gluteus Maximus	***Semi-membranosus***	***Adductor Magnus***
tendon length (l^t_s)	1.3979	1.1687	1.3799
muscle force (f^m_o)	0.2835	0.3681	0.2706
fiber length (l^m_o)	1.6851	2.2712	1.7989
tendon length + *muscle force*	1.1985 0.4582	1.0735 0.4980	0.8405 0.2540
muscle force + *fiber length*	0.5679 1.4216	0.5270 1.6179	0.2598 0.7687

Table 4: Minimal root-squared errors over the entire range of motion between the model predictions with optimal parameters and experimental data

Model Parameter	Muscle		
	Gluteus Maximus	***Semi-membranosus***	***Adductor Magnus***
tendon length	12.3378	26.7009	14.889
muscle force	10.6837	12.4913	5.6182
fiber length	1.6851	15.6517	16.4879
tendon length + *muscle force*	3.8984	11.5641	0.9181
muscle force + *fiber length*	3.2514	5.8355	1.3044